



Modified Porous Silicon with Zirconium Nanoparticles as a Selective Adsorbent for Phosphate Removal from Aqueous Systems

M. Anbia^{1*}, Z. Khodashenas¹ and L. Kamel²

¹Research Laboratory of Nanoporous Materials, Faculty of Chemistry, Iran University of Science and Technology, Tehran, Iran

²Faculty of Chemistry Iran University of Science and Technology Narmak, Tehran 16846-13114, Iran

PAPER INFO

Paper history:

Received 21 September 2018

Accepted in revised form 17 October 2018

Keywords:

Chemical etching

Porous silicon

Zirconium

Eutrophication

ABSTRACT

The development of an efficient adsorbent for phosphate removal from wastewater to prevent the eutrophication of surface waters is very important. In this study, porous silicon powder prepared with acidic etching solution (HF: HNO₃: H₂O). Then, Zirconium-modified porous silicon has been synthesized by a simple and low-cost hydrothermal process. The morphology and structure of the samples were investigated using scanning electron microscopy (SEM), X-ray diffraction (XRD). This material has been used as an adsorbent for phosphate ion (PO₄³⁻) removal from synthetic aqueous solutions. The effect of operating conditions such as contact time, initial anion concentration, pH, the presence of competitive ions on the adsorption performances and the regeneration of the adsorbent have been investigated. Maximum adsorption amount of 47.7 mg P/g has been obtained at ambient temperature. The maximum removal of phosphate was reached at pH= 4 for Zirconium-modified porous silicon. The adsorption was almost unaffected by the presence of competitive ions. Regeneration tests have shown that the adsorbent retains its capacity after 3 adsorption-desorption cycles.

doi: 10.5829/ijee.2018.09.03.05

INTRODUCTION

Eutrophication of aqueous systems by phosphate ions is one of the major environmental problem. The presence of phosphorous species in surface waters can lead to the abundant development of aquatic plants, the growth of algae, with some kinds of them being toxicogenic, thus causing eutrophication. Excessive increase in algae and decrease in water quality are the main results of eutrophication, which can lead to health problems and loss of property value [1–5]. The detergents used in industry and fertilizers from agricultural farming are the main pollution sources of phosphates in natural waters [6,7]. Phosphates are often present, in low concentrations in water, almost solely as organic phosphate, inorganic phosphate (orthophosphates) and polyphosphates [8].

A variety of methods for water treatment are available. Chemical and biological treatments are the most effective and well-established methods up to date, but they have some disadvantages such as operation difficulties and high cost at industrial level [2]. Various physicochemical methods have been suggested including reverse osmosis, electro-dialysis, contact filtration and adsorption [9–11]. The adsorption is a promising approach for the removal of pollutants because of simplicity and ease of operation. Furthermore, adsorption

capacity and selectivity could be improved by the surface modification of the adsorbent. Adsorption has been used as an alternative method for phosphate removal in wastewater treatment since 1960s which has some advantages, such as less production of sludge [10,12], low cost and easily available adsorbent materials [13].

Transition metal nanoparticles such as Zr, Al, Fe and etc. are capable of binding anionic ligands such as sulfate, nitrate, phosphate and arsenate [14–16]. Because sorption sites inhabit on the surface, these metals offer very high specific sorption capacity at nanoscale size due to their high surface area-to-volume ratio. The metal oxides are electron pair acceptors which can act as Lewis acids and are capable of selectively binding to Lewis bases. The phosphate anion as Lewis base donates electron pair(s) to form inner-sphere complexes by binding to the central metal atom of the metal oxide. Due to the high selectivity of zirconium oxide for phosphate, it can selectively adsorb phosphate from the background of other commonly occurring anions such as Cl⁻, SO₄²⁻ and NO₃⁻ because of these anions form only outer-sphere complexes with the surface of the metal oxide by Coulombic interactions [17]. Also, the complex of zirconium oxide and phosphate anion has high resistance against attacks by acids, alkalis, oxidants and reductants.

* Corresponding author: Mansoor Anbia
E-mail: anbia@iust.ac.ir

In the accumulated catalysts or adsorbents, pure metal is the active phase, but the metal nanoparticles show the strong tendency to agglomerate into larger ones. These results caused the negative effect on the effective surface area and removal performance. In addition, the separation and recycling of bare metal nanoparticles are extremely difficult and when used in their native form, lack the mechanical strength and attrition resistance properties that required for prolonged operation [18]. In supported catalysts or adsorbents, the active site located on a supporter which has a supporting role. The economic issue is an important reason for using supported catalysts or adsorbents because of metals such as platinum, iridium, etc. are expensive. Another reason to put active sites on the supporter is to make them available. The supporters have porous surface and allow the metal that used as an active site distributed in these areas and a more accessible surface [19]. To overcome these drawbacks, several solids such as graphite, zeolite, porous silica, carbon nanotube and alumina introduced as supporters or carriers of metal nanoparticles. Zirconium oxide is relatively high cost and applies pure zirconium oxide as an adsorbent is not cost-effective.

A Porous Silicon (PSi) was discovered more than 50 years ago; however, the interest of the scientific community on PSi has been only triggered in recent years. PSi possesses several interesting characteristics. Among its most significant characteristics are its very large specific area, high pore volume, uniform pore size distribution and controlled pore structure, the possibility to modify its pore size and morphology according to various requirements, as well as its biocompatibility and non-toxicity. Because of the unique properties of porous silicon, it was chosen as suitable substrate for the decoration of metal nanoparticles [20–23]. Also, PSi has photocatalytic activity in visible light [24]; so, it could be a suitable material for using in water treatment process.

The aim of this study was to investigate porous silicon functionalized with metal nanoparticles for the adsorptive removal of phosphate from aqueous solutions at a laboratory scale.

MATERIAL AND METHOD

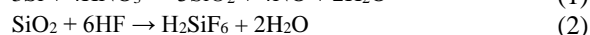
Chemicals

Polycrystalline Si powder (325 meshes, 99%), nitric acid (HNO₃) 65%, hydrofluoric acid (HF) 40%, ethanol, acetone, hydrochloric acid (HCl) 36.5%, zirconium oxychloride octahydrate (ZrOCl₂·8H₂O), paraffin, hydrogen peroxide (H₂O₂), sodium hydroxide (NaOH) and other chemicals were from Sigma-Aldrich and used without further purification. Anhydrous sodium dihydrogen phosphate (NaH₂PO₄) was from Merck (Germany). All solutions were prepared with deionized water (H₂O).

Synthesis of porous silicon

PSi powder was prepared via chemical etching, although other techniques, such as metal-assisted chemical etching and electrochemical etching, have been reported to produce PSi [25,26]. The technique used in this work is particularly simple and interesting because of the presence of readily available oxidizing and corrosive reagents; namely HNO₃ and H₂O, as well as HF [27]. For this purpose, 1.5 g of commercially Si powder with a mean particle size of 40 μm was dispersed in a mixture of HF: HNO₃: H₂O (4:3:6 volume ratio) in a plastic beaker. The mixture was stirred at 400 rpm for 80 min. During this time, the metallic color of the Si powder, converted to brown-yellow color, which indicated that the etching reaction was finished. The obtained PSi powder was filtered and the etched silicon powder was rinsed several times with deionized water to a neutral pH. Finally, the PSi powder was dried at 343K for 24 h and kept in a desiccator until further analysis.

Two-step chemical process performed for the etching of silicon in HF/HNO₃ mixtures including (i) the formal oxidation of silicon to SiO₂ by nitric acid (Eq. 1) and (ii) the subsequent dissolution of forming SiO₂ by HF (Eq. 2). The overall reaction, as written in Eq. 3, shows that formally only reaction products are water, nitrogen monoxide, and hexafluorosilicic acid [27].



Functionalization of porous silicon

The procedure described in the literature was followed to load zirconium oxide nanoparticles into the silicon powder [28]. 0.3g of zirconium oxychloride octahydrate was dissolved in 50mL of deionized water and then 1g of the porous silicon powder was added into this ZrOCl₂·8H₂O solution. Then, the suspension was stirred magnetically for 1.5 h. After that, 1M NaOH solution was slowly added dropwise to the suspension. During the addition of the NaOH solution, the suspension was stirred magnetically till the solution pH reached 10. After that, the suspension was stirred magnetically for 1h. Then the Zr-modified PSi was separated by filtration, washed repeatedly with deionized water, and finally dried in an oven at 80°C. The obtained dry material was stored in a desiccator for further use. Prior to use, the adsorbent was rinsed by 5% w NaCl solution to be converted into the chloride form, so as to minimize the pH variation during adsorption.

Characterization of the adsorbents

The morphology and the average diameter of the spheres were studied with scanning electron microscopy (SEM), obtained with a VEGA3 TESCAN microscope, operating at an accelerating voltage of 20 kV. The FTIR spectra of adsorbents were obtained by a Shimadzu 8400S Fourier transform infrared spectroscopy. The Zr contents in the

samples (chemical analysis) were obtained by Shimadzu AA-6300 atomic absorption spectrometer (AAS). The X-ray diffraction (XRD) analysis of adsorbent was performed with a Philips 1830 powder X-ray diffractometer. The concentration of phosphate was obtained with PG Instruments Ltd T80 ultraviolet-visible (UV-Vis) spectrophotometer by measuring the change in the absorption peak at 690 nm.

Adsorption studies

All adsorption experiments were carried out with batch method, at room temperature (298 ± 2 K) with a constant ionic strength of 0.01 M NaCl at pH= 6.1. The pH values of solutions were adjusted by adding 0.1M NaOH or 0.1M HCl solution. Some parameters such as metal content, adsorption time, pH and presence of competitive anions were varied for the phosphate adsorption studies. A phosphate stock solution of 100.0 mg/L used for the experiments was prepared by dissolving the anhydrous sodium dihydrogen phosphate, appropriate amounts of deionized water, without previous treatment. All the experiments were carried out by adding the appropriate amount of the adsorbent in 100 mL Erlenmeyer flasks containing 50.0 mL of the phosphate stock solution with concentration of 100.0 mg/L. The solutions were kept stirring on shaker bath at 400 rpm for an appropriate time. After the contact time, samples were filtered and the residual concentration of phosphate in the filtrates was determined by the stannous chloride method using a UV-Vis spectrophotometer [29–31]. Phosphate removal (R) was defined as:

$$(R)\% = 100 \times \frac{C_i - C_t}{C_i} \quad (4)$$

and the adsorption amount (mg P/g) was calculated as:

$$q_t = (C_i - C_t) \times \frac{V}{m} \quad (5)$$

Where C_i and C_t are the initial and final concentrations of the anion in solution (mg/L) respectively, q_t is the amount adsorbed at time t (mg P/g adsorbent), V is the solution volume (L), and m is the mass of adsorbent (g). The Effect of time, stirrer speed, initial phosphate concentration, pH, ion adsorption competitiveness were investigated to evaluate the phosphate removal using Zr modified PSi.

Desorption of phosphate from Zr modified PSi and reuse

To investigate the regenerability of Zr modified PSi, 0.1 g of adsorbent mixed with 50 mL of phosphate solution (100 ppm) for 90 min at 400 rpm, the adsorbent then was separated by filtration and concentration of phosphate was determined by UV-Vis. After filtration, the adsorbent was washed, dried at room temperature, and weighed. Then, anion loaded sample was stirred with different concentrations of NaOH solution 0.001, 0.01, 0.1 and 0.5 M for 30 min with a loading of 1 g adsorbent

to strip the phosphate anions. After filtration and washing with deionized water, the solid was dried at room temperature and weighed. The forward steps comprise first adsorption-desorption cycle, which was repeated by more cycles using the same adsorbent batch.

RESULTS AND DISCUSSION

Characterization of adsorbent

The morphology of the resulting PSi powder has been investigated and compared to bulk silicon powder. SEM images of the initial silicon powder and PSi powder after 80 min of etching are presented in Figure. 1. The surface of silicon powder is generally layered and smooth. In contrast, the surface of the PSi powder was rough, revealing pores. This indicates that etching of the silicon powder results in an increase in the surface area of the resulting PSi powder. Figure. 1(C and D) clearly indicate that the zirconium nanoparticles are well loaded on the PSi surface and have spherical morphology with increasing surface area, which is quite suitable for enhancing adsorption of phosphate.

The EDX spectra of Zr modified PSi before and after phosphate adsorption (Figure. 2) demonstrate that the nanocomposite consists of silicon and zirconium at concentration levels of 45.45 and 22.54%, respectively. These results indicate that the Zr/PSi nanocomposite has been successfully synthesized and phosphate ion is adsorbed.

The crystalline structures of the products were identified with XRD (Figure. 3). The diffraction peaks in silicon powder and PSi powder pattern ($2\theta = 28.4^\circ, 47.2^\circ, 56.4^\circ$,

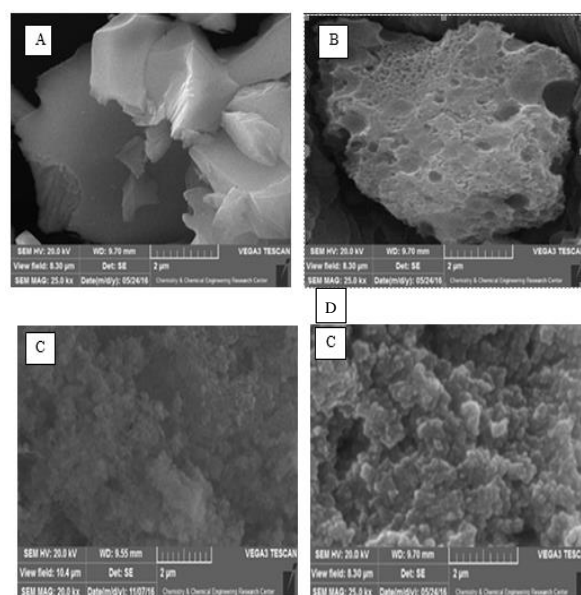


Figure 1. SEM images of (A) silicon powder, (B) porous silicon (PSi) powder after 80 min of etching, (C) and (D) Zr modified PSi powder

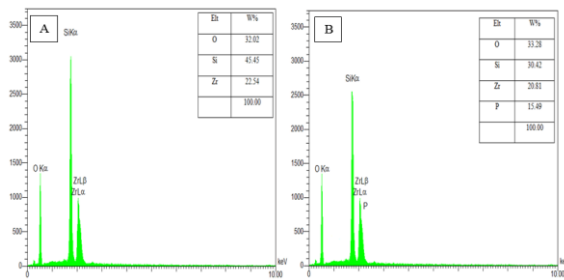


Figure 2. EDS spectra of Zr modified PSi powder before (A) and after (B) phosphate adsorption

69.4° and 76.6° can be assigned to Si (1 1 1), Si (2 2 0), Si (3 1 1), Si (4 0 0) and Si (3 3 1), respectively [32]. X-ray diffraction analysis shows that Zr nanoparticles loaded on PSi is poorly crystalline material and has nonuniform shapes. The results reveal that the presence of Zr nanoparticles on the outer surface of PSi powder has caused no change in the pattern, except that the overall intensity is reduced.

Figure 4 shows FT-IR spectra of the PSi in the wavenumber range of 400–4000 cm^{-1} . The absorption peak of PSi located at 610–620 cm^{-1} is assigned to Si–Si stretching modes and the peaks in the range of 1000–1300 cm^{-1} are corresponding to the stretching modes of the Si–O–Si groups [33]. The weak peaks in the range of 800–900 cm^{-1} show that the outermost surface of the PSi consists of SiH_2 species. The weak peaks in the range of 2000–2200 cm^{-1} show that the outermost surface of the PSi consists of SiH_x species [34]. The broad and intense band at 3450 cm^{-1} and the peak at 1630 cm^{-1} are possibly attributed to the stretching vibration and bending vibration of O–H groups, due to the structural hydroxyl group of SiOH and the presence of bound water or inhibited water [35]. It is found that Zr nanoparticles deposition on PSi causes no major change in the nature of the vibration modes or bonds present in PSi except in the reduction of overall intensity. After the phosphate adsorption, the FTIR spectrum of adsorbent demonstrates obvious changes. The peaks of physically adsorbed H_2O is greatly weakened. These observations indicate that the replacement of OH and H_2O has occurred during the phosphate adsorption. Additionally, new peaks appeared at 1037 cm^{-1} and 510–550 cm^{-1} , which are intensive. These new peaks could be assigned to the asymmetry vibration of P–O bonds, indicating that the surface hydroxyl groups have been replaced by the adsorbed phosphate ions [36].

Adsorption studies

Effect of time

The results of the effect of contact time for phosphate removal on PSi and Zr modified PSi are shown in Figure 5. From this Figure, it has been determined that 60 min of contact time is enough to reach the equilibrium and remove a considerable amount (47.7 mg/g) of phosphate

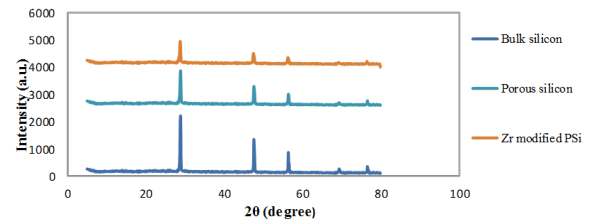


Figure 3. XRD patterns of bulk silicon powder and porous silicon powder

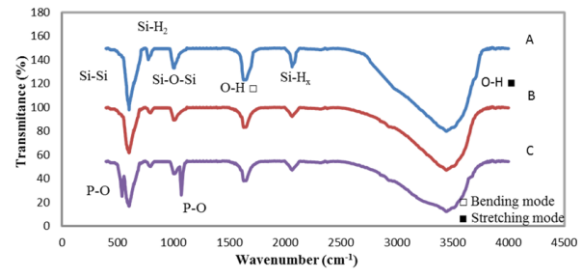


Figure 4. FT-IR spectra of PSi

present in aqueous solution. Further increase in contact time does not seem to have any impact on the equilibrium concentration. It is known that the time required to reach the equilibrium is short in the case of physical adsorption. The adsorption of phosphate into Zr modified PSi is a physical adsorption process occurring via electrostatic interactions between the positively charged surface zirconium groups and negatively charged phosphates anions in solution. When the Zr modified PSi surface (solid) is in contact with phosphate solution (liquid), the molecule of the liquid strikes the surface of the solid and the rate of adsorption is high as the whole surface is bare but as more and more of the system is covered, the available bare surface decreases and so does the rate of adsorption.

According to the study of adsorption kinetics, the adsorption results were fitted with the pseudo-second-order reaction kinetics expression [37]:

$$\frac{t}{q_t} = \left(\frac{1}{k_2 q_e^2} \right) + \left(\frac{1}{q_e} \right) t \quad (6)$$

where q_t is the sorption capacity at equilibrium at t (min); q_e is the sorption capacity at equilibrium (mg/g); k_2 (g/mg. min) is the equilibrium rate constant of pseudo-

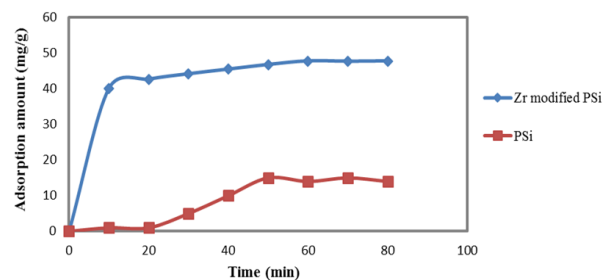


Figure 5. Adsorption of phosphate on Zr modified PSi as function of time

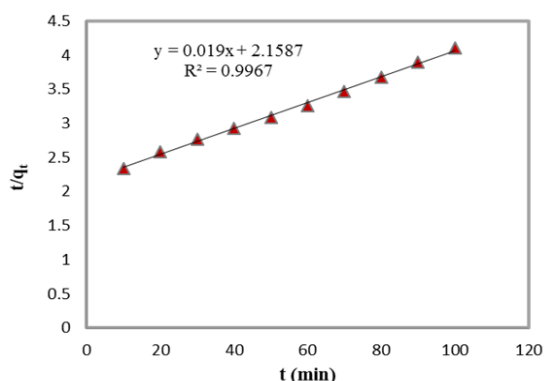


Figure 6. Pseudo-second order adsorption kinetics plots of t/q_t versus t using linear regression of Zr/PSi nanocomposite

second-order chemical sorption. In order to match experimental data with pseudo second order kinetics, t/q_e is plotted in terms of t . Figure. 6 shows, the high correlation coefficients (R^2) implied that dominant mechanism of the phosphate adsorption on Zr/PSi nanocomposite was chemisorption [38].

The adsorption isotherm can illustrate adsorption capacity at different phosphate equilibrium concentrations. Two isotherm models, the Langmuir and the Freundlich models are commonly described the adsorption process [39]. Langmuir equation is widely used to measure absorption capacity and is as follows [40]:

$$\frac{C_e}{q_e} = \frac{1}{q_m b} + \left(\frac{1}{q_m}\right)C_e \quad (7)$$

where C_e is equilibrium phosphate concentration (mg/L); q_e is equilibrium adsorption capacity (mgP/g of media); q_m (mg P/g) is the maximum phosphate adsorption capacity; b is the Langmuir adsorption isotherm constant related to the energy of adsorption (L/g). With the graph of C_e/q_e in the term, C_e can calculate b and q_m . The Langmuir isotherm describes the absorption process in which the active sites are uniform on the surface, so the species is absorbed homogeneously and single-layer on the surface. Freundlich isotherm is an experimental method that describes a state in which the species is absorbed by heterogeneous surface and expressed as follows [41,42]:

$$\ln(q_e) = \left(\frac{1}{n}\right) \ln C_e + \ln K_F \quad (8)$$

where K_F ($\text{mg}^{1-1/n} \text{L}^{1/n} \text{g}$) is the Freundlich dissociation constant, n is proportional to the intensity of the reaction. K_F and n determined from the linear plot of $\ln(q_e)$ versus $\ln C_e$. The values of the these equations constants obtained by linear regression analysis of the experimentally derived data are presented in Table 1 together with the correlation coefficient, R_2 . The higher value of correlation coefficient ($R_2 > 99$) on the Langmuir model compared to the R_2 value of the Freundlich model indicate Langmuir model is better fitted the phosphate adsorption behavior on the Zr/PSi.

TABLE 1. Langmuir and Freundlich constants for adsorption of phosphate on Zr/PSi.

Langmuir			Freundlich		
q_m (mg/g)	b (L/mg)	R^2	K_F	n (L/mg)	R^2
54.64	0.3552	0.9959	32.37	7.28	0.8580

Effect of agitation

Figure 7 illustrates the effect of stirrer speed on phosphate removal with Zr modified PSi. The results showed that upon increasing the stirring speed, adsorption capacity of phosphate does not change after 400 rpm, which means that phosphate ions could be diffused easily and quickly from the solution to the surface of the adsorbent without needing additional stirring.

Effect of initial phosphate concentration

The results are shown in Figure. 8. It can be seen that an increase in initial phosphate concentrations decreases the removal percentage of phosphate for the same adsorbent loading. This has been attributed to the higher initial concentration ratio of phosphate molecules to available surface area; therefore adsorption is dependent on initial concentration.

Effect of pH on phosphate removal

The effect of pH on phosphate removal is presented in Figure. 9. It is observed that the maximum phosphate

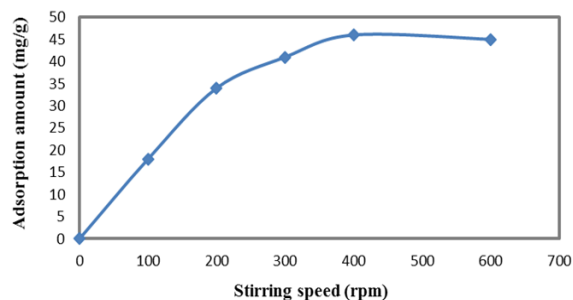


Figure 7. Effect of agitation on phosphate adsorption

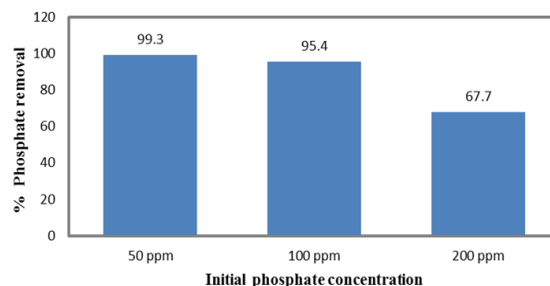


Figure 8. Effect of initial concentration on phosphate removal at 25°C

adsorption occurs at pH 4 (47.5 mg/g), and then it decreases gradually from pH 4 to pH 10. There are three forms of phosphate: H_2PO_4^- (dihydrogen phosphate anion), HPO_4^{2-} (hydrogen phosphate anion), or PO_4^{3-} (orthophosphate anion). The form of phosphate in the solution is dependent on the pH as described in Figure. 10 and Eqs. 9-1. H_2PO_4^- and HPO_4^{2-} species are present in the pH region between 4 and 10. The concentration of H_2PO_4^- species is higher at pH below 7 while predominate over PO_4^{3-} species while, for pH higher than 12.5 the concentration of PO_4^{3-} species becomes significant.



In this study, the higher removal of phosphate is expected at low pH values (corresponding to H_2PO_4^-) with increasing acidity of the solution $\text{pH} < \text{pK}_a$, the solution donates more protons than hydroxide groups (OH^-), and so the adsorbent surface is positively charged (attracting phosphate anions). Conversely, at higher $\text{pH} > \text{pK}_a$, the solution donates more hydroxide (OH^-), groups than H^+ and then surface charge of adsorbent becomes neutral losing electrostatic attraction towards the negatively charged phosphate anions HPO_4^{2-} and PO_4^{3-} [43]. The schematic of phosphate removal by Zr modified PSi showed in Figure. 11.

The immobilization of phosphate ions maybe occurs through the formation of inner or outer sphere surface complexes. The adsorption mechanisms of phosphate would describe with ion exchange (such as at low pH range) as follows (Eqs. 12 and 13):

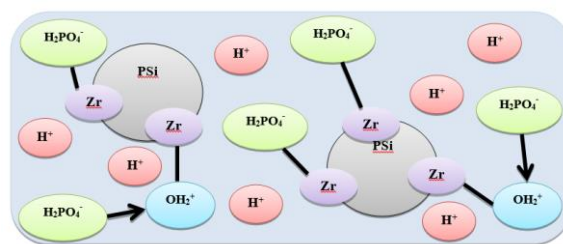
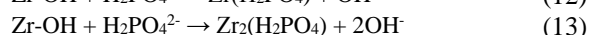
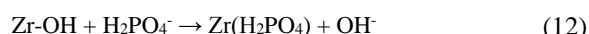
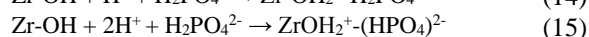


Figure 11. The schematic of phosphate removal by Zr modified PSi



And can explain with ligand exchange are given as[44-46]:



Effect of ion adsorption competitively

As shown in Table 2 and Figure. 12, the effect of competing ions on phosphate adsorption by Zr modified PSi has been found to follow this order $\text{Cl}^- < \text{NO}_3^- < \text{SO}_4^{2-}$. Apparently, sulfate ion just exhibit slight effect on phosphate removal by using Zr modified PSi. Phosphate has been considered to form inner-sphere complexes with metal oxides/hydroxides, whereas other ions often form outer-sphere complexes, which leads to ineffective competition. In general, effect of the presence of these ions on phosphate adsorption has not been significant.

TABLE 2. Effect of competing ions on phosphate removal by Zr modified PSi.

Existing ions	Phosphate removal %
H_2PO_4^- alone	95.4
$\text{H}_2\text{PO}_4^- + \text{Cl}^-$	93
$\text{H}_2\text{PO}_4^- + \text{NO}_3^-$	91.3
$\text{H}_2\text{PO}_4^- + \text{SO}_4^{2-}$	87

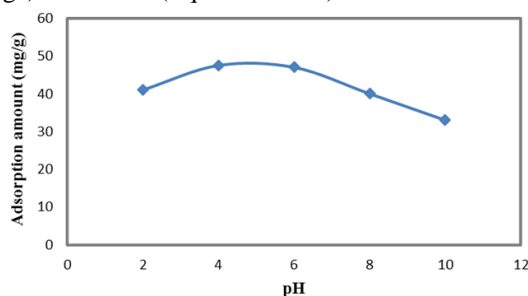


Figure 9. Effect pH on phosphate removal

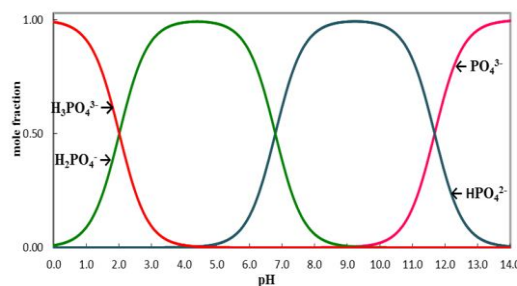


Figure 10. Distribution diagram for phosphate species as function of pH

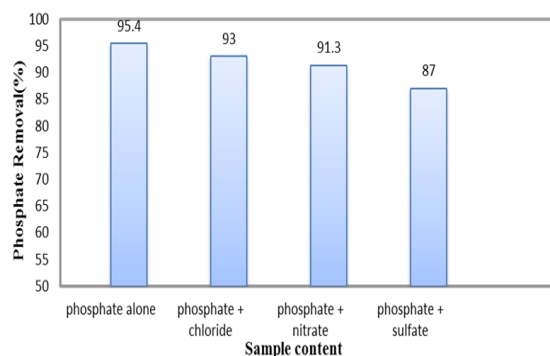


Figure 12. Effect of competing ions on phosphate removal by Zr modified PSi

Desorption of phosphate from Zr modified PSi

The phosphate adsorbed on Zr modified PSi could be desorbed with NaOH solution washing [43-48]. The performance of recovered adsorbent after first adsorption-desorption cycle are shown in Figure. 13. The percentage of phosphate removal is increased gradually with the increase of the alkalinity of NaOH solution. When the NaOH concentration is increased to 0.1 M, the phosphate removal percentage by recovered adsorbent also increased to 81.43%. When the NaOH concentration is increased to 0.5 M, it further increases to 91.25%. Results reveal that most of the phosphate adsorbed on Zr modified PSi could be easily desorbed using the NaOH solution with concentration at of 0.1 M or high. And this recovered adsorbent could be reuse for the phosphate removal from water to reduce the operation cost significantly. The spent Zr modified PSi is reused for further phosphate removal, which showed that they could maintain about 60–80% of its original phosphate removal capability after re-adsorption for three cycles. After last recycling, this material can use as fertilizer. The adsorbed phosphate transferred to the soil continuously in time. Also, concentrated and desorbed phosphate can be applied directly to the soil.

CONCLUSIONS

This study shows that Zr modified PSi synthesized from a simple and low-cost hydrothermal process demonstrates an effective phosphate removal performance in water. The adsorption performance is influenced by pH, initial phosphate concentration, stirring speed and co-existing anions. The maximum adsorption amount of phosphate was determined at about 47.7 mg/g at pH 6.1, which was among the highest reported values in the literature. The adsorption mechanism of phosphate onto Zr modified PSi has been determined to follow the inner-sphere complexation mechanism, and the surface -OH groups play the main role in phosphate removal. In general, different interactions such as electrostatic, Lewis acid-base

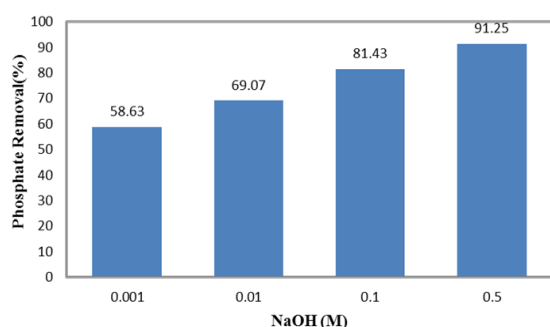


Figure 13. Phosphate removal by recovered Zr modified PSi using NaOH solutions with different concentrations from 0.001 to 0.5 M

interactions and ion exchange between the loading groups on the adsorbents and the phosphate anion is, reported for the phosphate adsorption of metal oxides. Zr modified PSi could remove phosphate effectively even when competing anions are present. Thus, it has the potential to be a promising adsorbent for the phosphate removal. Furthermore, catalytic feature of PSi in visible light could have a positive effect in water treatment.

ACKNOWLEDGMENT

The authors are thankful to the Research Council of the Iran University of Science and Technology for its financial support of the present research work.

REFERENCES

1. Cao, D., X. Jin, L. Gan, T. Wang and Z. Chen, 2016. Removal of phosphate using iron oxide nanoparticles synthesized by eucalyptus leaf extract in the presence of CTAB surfactant. *Chemosphere*, 159: 23–31.
2. Liu, X. and L. Zhang, 2015. Removal of phosphate anions using the modified chitosan beads: adsorption kinetic, isotherm and mechanism studies. *Powder Technology*, 277: 112–119.
3. Li, R., J.J. Wang, B. Zhou, M.K. Awasthi, A. Ali, Z. Zhang, L.A. Gaston, A.H. Lahori and A. Mahar, 2016. Enhancing phosphate adsorption by Mg/Al layered double hydroxide functionalized biochar with different Mg/Al ratios. *Science of the Total Environment*, 559: 121–129.
4. Lai, L., Q. Xie, L. Chi, W. Gu and D. Wu, 2016. Adsorption of phosphate from water by easily separable Fe₃O₄@SiO₂ core/shell magnetic nanoparticles functionalized with hydrous lanthanum oxide. *Journal of Colloid and Interface Science*, 465: 76–82.
5. Nouri, H., S. Chavoshi Borujeni, R. Nirola, A. Hassanli, S. Beecham, S. Alaghmand, C. Saint and D. Mulcahy, 2017. Application of green remediation on soil salinity treatment: A review on halophytoremediation. *Process Safety and Environmental Protection*, 107: 94–107.
6. Song, L., J. Huo, X. Wang, F. Yang, J. He and C. Li, 2016. Phosphate adsorption by a Cu (II)-loaded polyethersulfone-type metal affinity membrane with the presence of coexistent ions. *Chemical Engineering Journal*, 284: 182–193.
7. Zelmanov, G. and R. Semiat, 2015. The influence of competitive inorganic ions on phosphate removal from water by adsorption on iron (Fe³⁺) oxide/hydroxide nanoparticles-based agglomerates. *Journal of Water Process Engineering*, 5: 143–152.
8. Wang, W., C. Ma, Y. Zhang, S. Yang, Y. Shao and

- X. Wang, 2016. Phosphate adsorption performance of a novel filter substrate made from drinking water treatment residuals. *Journal of Environmental Sciences*, 45: 191–199.
9. Esfandiyari, T., N. Nasirizadeh, M. Dehghani and M.H. Ehrampoosh, 2017. Graphene oxide based carbon composite as adsorbent for Hg removal: Preparation, characterization, kinetics and isotherm studies. *Chinese Journal of Chemical Engineering*, 25(9): 1170–1175.
 10. Zong, E., X. Liu, J. Jiang, S. Fu and F. Chu, 2016. Preparation and characterization of zirconia-loaded lignocellulosic butanol residue as a biosorbent for phosphate removal from aqueous solution. *Applied Surface Science*, 387: 419–430.
 11. Anbia, M., A. Sedighi and S. Salehi, 2016. *Iranica Journal of Energy & Environment. Energy and Environment*, 7(3): 221–225.
 12. Lu, J., H. Liu, X. Zhao, W. Jefferson, F. Cheng and J. Qu, 2014. Phosphate removal from water using freshly formed Fe--Mn binary oxide: adsorption behaviors and mechanisms. *Colloids and Surfaces A: Physicochemical and Engineering Aspects*, 455: 11–18.
 13. Wang, Z., D. Shen, F. Shen and T. Li, 2016. Phosphate adsorption on lanthanum loaded biochar. *Chemosphere*, 150: 1–7.
 14. Johir, M.A.H., M. Pradhan, P. Loganathan, J. Kandasamy and S. Vigneswaran, 2016. Phosphate adsorption from wastewater using zirconium (IV) hydroxide: kinetics, thermodynamics and membrane filtration adsorption hybrid system studies. *Journal of Environmental Management*, 167: 167–174.
 15. Soliemanzadeh, A. and M. Fekri, 2017. Synthesis of clay-supported nanoscale zero-valent iron using green tea extract for the removal of phosphorus from aqueous solutions. *Chinese Journal of Chemical Engineering*, 25(7): 924–930.
 16. Saberi, A., 2012. Comparison of Pb removal efficiency by zero valent iron 2+ nanoparticles and Ni/Fe bimetallic nanoparticles. *J. Energy Environ*, 3(2): 189–196.
 17. Acelas, N.Y., B.D. Martin, D. López and B. Jefferson, 2015. Selective removal of phosphate from wastewater using hydrated metal oxides dispersed within anionic exchange media. *Chemosphere*, 119: 1353–1360.
 18. Blaney, L.M., S. Cinar and A.K. SenGupta, 2007. Hybrid anion exchanger for trace phosphate removal from water and wastewater. *Water Research*, 41(7): 1603–1613.
 19. Anbia, M. and M. Rezaie, 2017. Generation of sulfate radicals by supported ruthenium catalyst for phenol oxidation in water. *Research on Chemical Intermediates*, 43(1): 245–257.
 20. Kovacs, A. and U. Mescheder, 2012. Transport mechanisms in nanostructured porous silicon layers for sensor and filter applications. *Sensors and Actuators B: Chemical*, 175: 179–185.
 21. Dimova-Malinovska, D., M. Sendova-Vassileva, N. Tzenov and M. Kamenova, 1997. Preparation of thin porous silicon layers by stain etching. *Thin Solid Films*, 297(1): 9–12.
 22. Beale, M.I.J., J.D. Benjamin, M.J. Uren, N.G. Chew and A.G. Cullis, 1986. THE FORMATION OF POROUS SILICON BY CHEMICAL STAIN ETCHES M.I.J. BEALE, J.D. BENJAMIN, M.J. UREN, N.G. CHEW and A.G. CULLIS. *Journal of Crystal Growth*, 75: 408–414.
 23. Halim, M.Y.A., W.L. Tan, N.H.H.A. Bakar and M.A. Bakar, 2014. Surface characteristics and catalytic activity of copper deposited porous silicon powder. *Materials*, 7(12): 7737–7751.
 24. Kamel, L. and M. Anbia, 2017. Preparation and evaluation of nanoporous-pyramids structured silicon powder as an effective photocatalyst for degradation of methyl red. *International Journal of Environmental Science and Technology*, 1–8.
 25. Maniya, N.H., S.R. Patel and Z.V.P. Murthy, 2013. Electrochemical preparation of microstructured porous silicon layers for drug delivery applications. *Superlattices and Microstructures*, 55: 144–150.
 26. Li, X. and P.W. Bohn, 2012. Metal-assisted chemical etching in HF / H₂ O₂ produces porous silicon Metal-assisted chemical etching in HF / H₂ O₂ produces porous silicon. 2572(2000): 28–31.
 27. Ensafi, A.A., F. Rezaloo and B. Rezaei, 2016. Electrochemical sensor based on porous silicon/silver nanocomposite for the determination of hydrogen peroxide. *Sensors and Actuators B: Chemical*, 231: 239–244.
 28. Yang, M., J. Lin, Y. Zhan and H. Zhang, 2014. Adsorption of phosphate from water on lake sediments amended with zirconium-modified zeolites in batch mode. *Ecological Engineering*, 71: 223–233.
 29. APHA, AWWA. "WPCF, 1992 Standard Methods for the Examination of Water and Wastewater." (1988): 801-823.
 30. APHA, Water Environment Federation and American Water Works Association, 1999. Standard Methods for the Examination of Water and Wastewater Part 4000 Inorganic Nonmetallic Constituents Standard Methods for the Examination of Water and Wastewater. Standard Methods for the Examination of Water and Wastewater, 733.
 31. Lim, S., 1991. Determination of phosphorus concentration in hydroponics solution. *Methodology*, 1–4.
 32. Westra, J.M., V. Vavruňková, P. Šutta, R.A.C.M.M. Van Swaaij and M. Zeman, 2010. Formation of thin-film crystalline silicon on glass observed by in-situ XRD. *Energy Procedia*, 2(1): 235–241.

33. Mawhinney, D.B., J.A. Glass and J.T. Yates, 1997. FTIR study of the oxidation of porous silicon. The Journal of Physical Chemistry B, 101(7): 1202–1206.
34. Azodi, M., C. Falamaki and A. Mohsenifar, 2011. Journal of Molecular Catalysis B: Enzymatic Sucrose hydrolysis by invertase immobilized on functionalized porous silicon. "Journal of Molecular Catalysis. B, Enzymatic," 69(3–4): 154–160.
35. Khalifa, M., M. Hajji and H. Ezzaouia, 2012. Purification of silicon powder by the formation of thin porous layer followed by photo-thermal annealing. Nanoscale Research Letters, 7(1): 444. <https://doi.org/10.1186/1556-276X-7-444>
36. Coulibaly, L.S., S.K. Akpo, J. Yvon and L. Coulibaly, 2016. Fourier transform infra-red (FTIR) spectroscopy investigation, dose effect, kinetics and adsorption capacity of phosphate from aqueous solution onto laterite and sandstone. Journal of Environmental Management, 183: 1032–1040.
37. Ho, Y.-S. and G. McKay, 1998. Sorption of dye from aqueous solution by peat. Chemical Engineering Journal, 70(2): 115–124.
38. Ho, Y.-S. and G. McKay, 2000. The kinetics of sorption of divalent metal ions onto sphagnum moss peat. Water Research, 34(3): 735–742.
39. Kovo, A., S. Olu and E. Gwatana, 2014. Adsorption of chromium (IV) by a low cost adsorbent prepared from Neem leaves. Iranica J. of Energy & Environment, 5(3): 277–286.
40. Langmuir, I., 1916. The constitution and fundamental properties of solids and liquids. Part I. Solids. Journal of the American Chemical Society, 38(11): 2221–2295.
41. Freundlich, H.M.F. and others, 1906. Over the adsorption in solution. J. Phys. Chem, 57(385471): 1100–1107.
42. Bouamra, F., N. Drouiche, N. Abdi, H. Grib, N. Mameri and H. Lounici, Removal of Phosphate from Wastewater by Adsorption on Marble Waste: Effect of Process Parameters and Kinetic Modeling. International Journal of Environmental Research, 1–15.
43. Harris, D.C., 2010. Quantitative chemical analysis. Macmillan.
44. Chitrakar, R., S. Tezuka, A. Sonoda, K. Sakane, K. Ooi and T. Hirotsu, 2006. Selective adsorption of phosphate from seawater and wastewater by amorphous zirconium hydroxide. Journal of Colloid and Interface Science, 297(2): 426–433.
45. Luo, X., X. Wang, S. Bao, X. Liu, W. Zhang and T. Fang, 2016. Adsorption of phosphate in water using one-step synthesized zirconium-loaded reduced graphene oxide. Scientific Reports, 6: 39108.
46. Zong, E., D. Wei, H. Wan, S. Zheng, Z. Xu and D. Zhu, 2013. Adsorptive removal of phosphate ions from aqueous solution using zirconia-functionalized graphite oxide. Chemical Engineering Journal, 221: 193–203.
47. Han, B., N. Chen, D. Deng, S. Deng, I. Djerdj and Y. Wang, 2015. Enhancing phosphate removal from water by using ordered mesoporous silica loaded with samarium oxide. Analytical Methods, 7(23): 10052–10060.
48. Chitrakar, R., S. Tezuka, A. Sonoda, K. Sakane, K. Ooi and T. Hirotsu, 2006. Phosphate adsorption on synthetic goethite and akaganeite. Journal of Colloid and Interface Science, 298(2): 602–608.

Persian Abstract

DOI: 10.5829/ijee.2018.09.03.05

چکیده

ظهور یک جاذب کارآمد برای حذف فسفات از فاضلاب برای جلوگیری از تخریب آب‌های سطحی بسیار مهم است. در این مطالعه، پودر سیلیکون متخلخل با محلول حکاکی اسیدی (HF:HNO₃:H₂O) تهیه شد. سپس سیلیکون متخلخل اصلاح شده با زیرکونیم توسط فرآیند ساده و کم هزینه هیدروترمال ساخته شده است. مورفولوژی و ساختار نمونه‌ها با استفاده از میکروسکوپ الکترونی روبشی (SEM)، پراش اشعه ایکس (XRD) مورد بررسی قرار گرفت. این ماده به عنوان یک جاذب برای حذف یون فسفات (PO₄³⁻) از محلول‌های آبی ساخته شده استفاده شده است حداکثر جذب مقدار 47/7 میلی گرم فسفر بر گرم در دمای محیط بدست آمد. حداکثر حذف فسفات در pH=4 برای سیلیکون متخلخل اصلاح شده با زیرکونیوم به دست آمد. جذب تقریباً تحت تاثیر یونهای رقابت کننده قرار نگرفت. آزمایش‌های بازسازی نشان داده است که جاذب ظرفیت خود را پس از 3 بار جذب-وا جذب حفظ می‌کند.
